Catalysis Today 147 (2009) 150–157

Contents lists available at ScienceDirect

Catalysis Today

journal homepage: www.elsevier.com/locate/cattod

Comparison of H_2 production from ethanol and ethylene glycol on M/Pt(1 1 1) (M = Ni, Fe, Ti) bimetallic surfaces

Orest Skoplyak, Mark A. Barteau, Jingguang G. Chen *

Center for Catalytic Science and Technology, Department of Chemical Engineering, University of Delaware, Newark, DE 19716, United States

ARTICLE INFO

Article history:
Available online 17 January 2009

Keywords:
Pt(1 1 1)
Ni
Fe
Ti
Ethylene glycol
Ethanol
Bimetallic surface
TPD
H_2 production
d-Band center

ABSTRACT

The reactions of ethylene glycol and ethanol have been studied on Fe/Pt(1 1 1) and Ti/Pt(1 1 1) bimetallic surfaces utilizing temperature programmed desorption (TPD). These results are compared to our previous studies on Ni/Pt(1 1 1) to illustrate the trend in the reforming activity on 3d-Pt bimetallic surfaces. The oxygenates decomposed on these surfaces to produce mainly H_2 and CO. The bimetallic surfaces were prepared by thermal evaporation of Fe or Ti onto Pt(1 1 1), using Auger electron spectroscopy (AES) to monitor surface compositions. Surfaces prepared by deposition of a monolayer of Fe or Ti on Pt(1 1 1), designated Fe–Pt–Pt(1 1 1) or Ti–Pt–Pt(1 1 1), displayed higher reforming activity for both ethylene glycol and ethanol than the corresponding subsurface monolayer Pt–Fe–Pt(1 1 1) and Pt–Ti–Pt(1 1 1) structures or clean Pt(1 1 1). The reforming yield increased as the surface d-band center, calculated from density functional theory (DFT), shifted closer to the Fermi level. The reforming selectivity of oxygenates, especially ethanol, began to decrease as the d-band center shifted closer to the Fermi level. Combining results in the current work with previous studies on Ni/Pt(1 1 1), a general criterion can be formulated for selecting 3d-Pt bimetallic surfaces with desirable reforming activity and selectivity.

1. Introduction

Selective reforming of oxygenates can be used for the production of hydrogen for use in fuel cells. If the oxygenates are derived from renewable biomass the reforming process is potentially CO_2 neutral, as the CO_2 by-product can be consumed by future biomass growth. Other advantages of oxygenate reforming include low toxicity and low reactivity of the reactants, which are compatible with the current infrastructure for transportation and storage. A general review on this topic can be found in a recent paper by Dumesic and co-workers [1,2]. Along with use of oxygenates for production of hydrogen, the direct use of methanol [3–5], ethanol [6–8] and ethylene glycol [9,10] in fuel cells has attracted recent attention, as new catalytic materials are needed to increase the kinetics of oxygenate oxidation at the anode.

The reforming of an oxygenate, using ethylene glycol as an example, can be described as follows. The reaction proceeds through initial dehydrogenation and C–C bond scission to produce CO and H_2. CO further reacts with H_2O through the water gas shift reaction to produce CO_2 and more H_2. The overall reaction produces CO_2 and H_2.

$$C_2O_2H_6 \rightarrow 2CO + 3H_2$$

$$CO + H_2O \rightarrow CO_2 + H_2$$

$$C_2O_2H_6 + 2H_2O \rightarrow 2CO_2 + 5H_2$$

This study focuses on the initial oxygenate dehydrogenation and C–C bond scission, which will be referred to as reforming throughout the paper.

In our previous work, the reforming of ethylene glycol and ethanol was studied on Ni/Pt(1 1 1) bimetallic surfaces [11,12]. The surface with a monolayer of Ni atoms residing on Pt(1 1 1), designated as Ni–Pt–Pt(1 1 1), displayed increased activity for reforming of ethanol and ethylene glycol. A linear correlation between experimental reforming yield and the surface d-band center calculated by DFT was observed, with increasing yield as the surface d-band center shifted closer to the Fermi level. Similar increases in reforming activity on the Ni–Pt–Pt(1 1 1) surface have been observed using methanol [13] and glycerol [14] as probe reagents. Along with surface science studies, investigations using supported catalysts showed that NiPt, CoPt, and FePt supported on γ-Al_2O_3 displayed increased turnover frequencies for aqueous

* Corresponding author.
E-mail address: jgchen@udel.edu (J.G. Chen).

0920-5861/$ – see front matter © 2008 Elsevier B.V. All rights reserved.
doi:10.1016/j.cattod.2008.12.005

phase reforming of ethylene glycol compared to Pt/γ-Al_2O_3 at similar conditions [15].

The different properties of the surface monolayer, 3d-Pt–Pt(1 1 1), versus the subsurface monolayer structure, Pt-3d-Pt(1 1 1), have been investigated using a series of 3d metals, including Ni, Co, Fe, and Cu [16,17]. The Pt-3d-Pt(1 1 1) surfaces exhibit decreased interactions with adsorbates, such as atomic hydrogen and oxygen, and molecularly adsorbed alkenes, compared to those on the 3d-Pt–Pt(1 1 1) surfaces. The weaker binding energy of atomic hydrogen is important for low temperature hydrogenation activity, while stronger binding energies are of interest for reforming reactions. The experimental results are in agreement with previous theoretical DFT studies [18–22] of binding energies of atomic and molecular adsorbates.

The reactions of ethylene glycol have been previously studied on Pt(1 1 1) [11], Cu(1 1 0) [23], Ni(1 0 0) [24], Ag(1 1 0) [25,26], Rh(1 1 1) [27], and Mo(1 1 0) [28]. Ethanol has been studied previously on many surfaces, including Pt(1 1 1) [11,29–31], and Ni(1 1 1) [32,33]. In this work, we investigate the reforming of ethylene glycol and ethanol on Fe/Pt(1 1 1) and Ti/Pt(1 1 1) bimetallic surfaces, and compare these results with our previous studies on Ni/Pt(1 1 1) to correlate the trends in reforming activity and selectivity as a function of surface d-band center. The comparison reveals that the 3d-Pt–Pt(1 1 1) structure is more active compared to the Pt-3d-Pt(1 1 1) structure for Ni, Fe and Ti bimetallic surfaces. Reforming activity generally increases for surfaces with d-band centers closer to the Fermi level. However, reforming selectivity decreases for early transition metal bimetallic surfaces such as Ti/Pt(1 1 1), suggesting that optimal catalysts for reforming would contain Ni, Co and Fe on Pt(1 1 1).

2. Experimental

The UHV chamber used for the experiments was a two-level stainless steel chamber (base pressure of 1×10^{-10} Torr), equipped for Auger electron spectroscopy (AES) and temperature programmed desorption (TPD). TPD experiments were performed using a quadrupole mass spectrometer (UTI 100C), which could monitor up to 12 masses simultaneously. A linear rate of 3 K/s was used in all TPD measurements. The Pt(1 1 1) single crystal (Princeton Scientific, 99.99%) was 1 mm thick, with a 10 mm diameter, and was oriented to within 0.5°. The crystal was spot-welded directly to two tantalum posts that served as electrical connections for resistive heating, as well as thermal contacts for cooling with liquid nitrogen. The temperature of the crystal could be varied between 100 K and 1100 K, and was measured by spot welding a chromel-alumel thermocouple to the top edge of the Pt(1 1 1) single crystal. The Pt(1 1 1) surface was cleaned by repeated cycles of Ne^+ sputtering at 600 K and annealing at 1100 K. Following the last sputter cycle, 1 L of O_2 at 890 K was used to remove carbon left on the surface, followed by annealing at 1100 K for 5 min. This cleaning procedure was repeated until negligible C or O was detected by AES.

Ethylene glycol (Sigma–Aldrich, 99.8%) and ethanol (Sigma–Aldrich, 99.5+%) were transferred into glass sample cylinders and purified using repeated freeze-pump-thaw cycles. All other gases were of research purity and were used without further purification. The purity of all reagents was verified in situ by mass spectrometry prior to use. Doses are reported in Langmuirs ($1\ L = 1 \times 10^{-6}$ Torr s) and are uncorrected for ion gauge sensitivity or flux enhancement due to dosing with the directional doser. In all experiments, the gas exposures were made at a crystal temperature of 200 K through a 1/4 in. stainless steel tube. For ethylene glycol experiments, dosing was performed with the crystal several inches away facing the dosing tube. Ethanol experiments were performed with the crystal facing away from the dosing tube.

The Fe/Pt(1 1 1) and Ti/Pt(1 1 1) bimetallic surfaces were prepared by thermal evaporation of Fe or Ti onto a Pt(1 1 1) single crystal, similar to procedures described earlier for Ni and Co [18,34]. The source consisted of a tungsten filament with a high purity Fe or Ti wire (Alfa Aesar, 99.99+%) wrapped around it, mounted within a tantalum enclosure. AES was used to monitor surface composition. For Fe/Pt(1 1 1) surfaces, the Fe(654 eV)/Pt(241 eV) AES ratio was used to determine Fe coverages, where a Fe/Pt ratio of 0.8 was taken as the monolayer coverage for Pt–Fe–Pt(1 1 1) based on previous calibration [16]. The Pt–Fe–Pt(1 1 1) surface was prepared at a crystal temperature of 600 K, while for Fe–Pt–Pt(1 1 1) a temperature of 300 K was used. For preparation of Ti/Pt(111) surfaces the Ti(421 eV)/Pt(241 eV) AES ratio was used to determine Ti coverage. Further explanation of Ti deposition and surface characterization will be presented in Section 3.

3. Results

3.1. Brief summary of reforming on Ni/Pt(1 1 1)

TPD experiments have shown that the Ni–Pt–Pt(1 1 1) surface exhibits increased reforming activity compared to either Ni(1 1 1) film, Pt(1 1 1), or Pt–Ni–Pt(1 1 1) surfaces for oxygenates such as methanol, ethanol, ethylene glycol, and glycerol [11,13,14]. The reforming activity displays a linear trend with the surface d-band center, increasing as the d-band center shifts closer to the Fermi level. Results from the Ni/Pt(1 1 1) system suggest that for reforming reactions surfaces with d-band center closer to the Fermi level are desired, and this can be achieved by placing 3d metal on the surface of Pt(1 1 1). Furthermore, the d-band center of 3d-Pt–Pt(1 1 1) shifts closer to the Fermi level as the 3d metal moves toward left side of the Periodic Table. The primary focus of the current paper is to test such predictions using the Fe/Pt(1 1 1) and Ti/Pt(1 1 1) surfaces. In order to explore other 3d/Pt(1 1 1) surfaces that might be promising for the reforming chemistry, the binding energies of ethanol and ethoxy were calculated on other surface monolayer Pt-based bimetallic surfaces, using 3d metals as the surface monolayer starting from Ni all the way to Ti, as shown in Fig. 1. Adsorbed species were bound in the atop configuration, with calculation details similar to those described for the Ni/Pt(1 1 1) surfaces [12]. Previous results for methanol and methoxy on Ni/Pt(1 1 1) and Co/Pt(1 1 1) [13] are also included for comparison. The binding energies increased as the d-band center moved closer to the Fermi level, and this could be achieved by choosing the surface 3d metal from the left side of the Periodic Table. The binding energies of the alkoxide species were greater than those of the molecular species. As seen from the trend, the 3d-Pt–Pt(1 1 1) surface structures should be promising for reforming of oxygenates, as the reforming activity is expected to increase as the binding energy increases. However, an optimal binding energy is likely needed, as surfaces with very strong binding energy are more likely to react by total decomposition, decreasing the reforming selectivity, as shown below for the reactions of ethanol and ethylene glycol on Fe/Pt(1 1 1) and Ti/Pt(1 1 1) surfaces.

3.2. Ethylene glycol TPD on Fe/Pt(1 1 1)

TPD experiments were conducted to probe the reactivity of different bimetallic surfaces for oxygenate reforming. Ethylene glycol is an ideal probe molecule for reforming, as its 1:1 C:O stoichiometry leads to the production of only CO and H_2 in the reforming reaction. It is also the smallest molecule with OH groups attached to adjacent carbons, a structural feature found in oxygenates derived from carbohydrates, such as glycerol, sorbitol, glucose, etc.

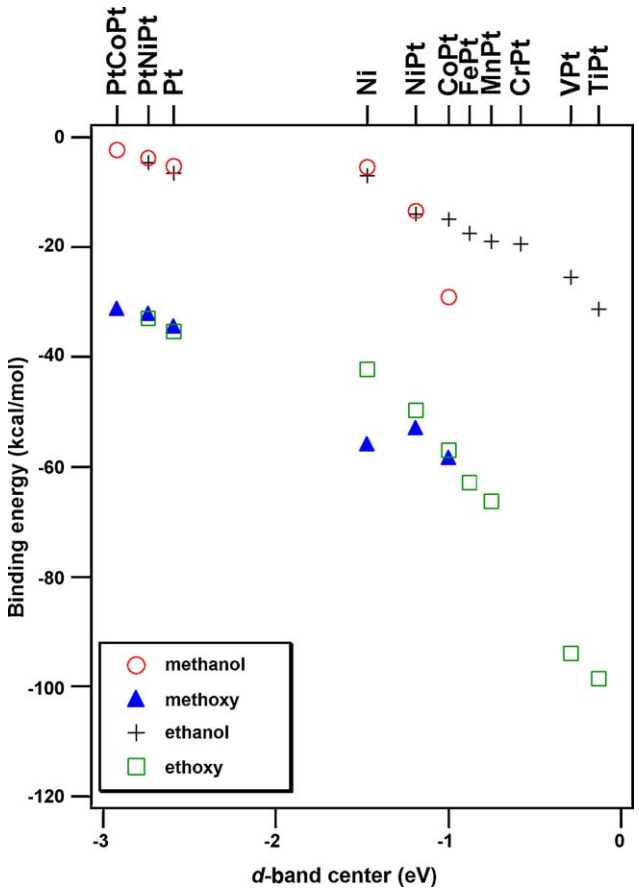

Fig. 1. DFT calculated binding energies of methanol, methoxy, ethanol, and ethoxy on 3d-Pt–Pt(1 1 1) bimetallic surfaces.

Fig. 2 displays the TPD spectra of (a) ethylene glycol, (b) H_2 and (c) CO following 0.2 L ethylene glycol exposure on Fe/Pt(1 1 1) bimetallic surfaces. Ethylene glycol desorbed from Fe/Pt(1 1 1) bimetallic surfaces from two peaks with the same peak temperatures as on clean Pt(1 1 1). The lower temperature peak at 226 K was attributed to multilayer desorption, while the peak at 266 K was attributed to monolayer desorption. On Pt(1 1 1) the H_2 and CO products desorbed at 328 K and 461 K, respectively, both consistent with desorption-limited processes. From Pt–Fe–Pt(1 1 1), H_2 and CO desorbed at 305 K and 413 K, respectively, both at lower peak temperatures compared to clean Pt(1 1 1). From Fe–Pt–Pt(1 1 1), H_2 desorbed from several peaks. A low temperature peak was observed at 313 K, followed by high temperature overlapping peaks at 417 K and 443 K. The high temperature peak was reaction-limited, as the desorption temperature was higher than that following H_2 adsorption on this surface (spectrum not shown). CO desorption occurred at 443 K, with a low temperature shoulder at 413 K. Comparing peak areas among the three surfaces, Fe–Pt–Pt(1 1 1) displayed increased H_2 and CO peak areas compared to Pt(1 1 1), although the increase was not as significant as for the Ni–Pt–Pt(1 1 1) surface reported previously [11]. Pt–Fe–Pt(1 1 1) also showed increased CO peak areas as compared to Pt(1 1 1), in contrast to previous results for Pt–Ni–Pt(1 1 1) relative to Pt(1 1 1) [11].

3.3. Ethanol TPD on Fe/Pt(1 1 1)

Ethanol was used as a probe molecule, as it has attracted interest as renewable fuel to produce H_2 for hydrogen fuel cells or for direct use in ethanol fuel cells [6–8]. The 2:1 C:O stoichiometry of ethanol leads to the deposition of carbon on the surface along with CO and H_2. The surface carbon can be removed with water by steam reforming.

TPD spectra of (a) ethanol, (b) H_2 and (c) CO following 0.3 L ethanol exposures on Fe/Pt(1 1 1) bimetallic surfaces are shown in Fig. 3. The results on Pt(1 1 1) were in good agreement with previous studies [11,29–31]. Ethanol desorbed from Pt(1 1 1) at 220 K, and from Pt–Fe–Pt(1 1 1) and Fe–Pt–Pt(1 1 1) surfaces at 232 K and 260 K, respectively. All peaks were attributed to monolayer desorption, as ethanol multilayer desorption occurred at ~175 K and was not observed here because ethanol was dosed on the surface at 200 K. Comparing peak areas, the ethanol peak on Fe–Pt–Pt(1 1 1) was significantly reduced compared to the other two surfaces. Ethanol reacted on Fe/Pt(1 1 1) bimetallic surfaces to form mainly H_2 and CO as the gas-phase products. Small amounts of CH_4 (not shown) were observed on Pt(1 1 1), but not on Fe/Pt(1 1 1) surfaces. H_2 desorbed from Pt–Fe–Pt(1 1 1) from several peaks centered at 286 K, 319 K, and 375 K. From Fe–Pt–Pt(1 1 1), H_2 desorbed from peaks at 319 K, 367 K and 414 K. CO desorption occurred at 421 K and 416 K from Pt–Fe–Pt(1 1 1) and Fe–Pt–Pt(1 1 1) surfaces, respectively, both lower than from clean

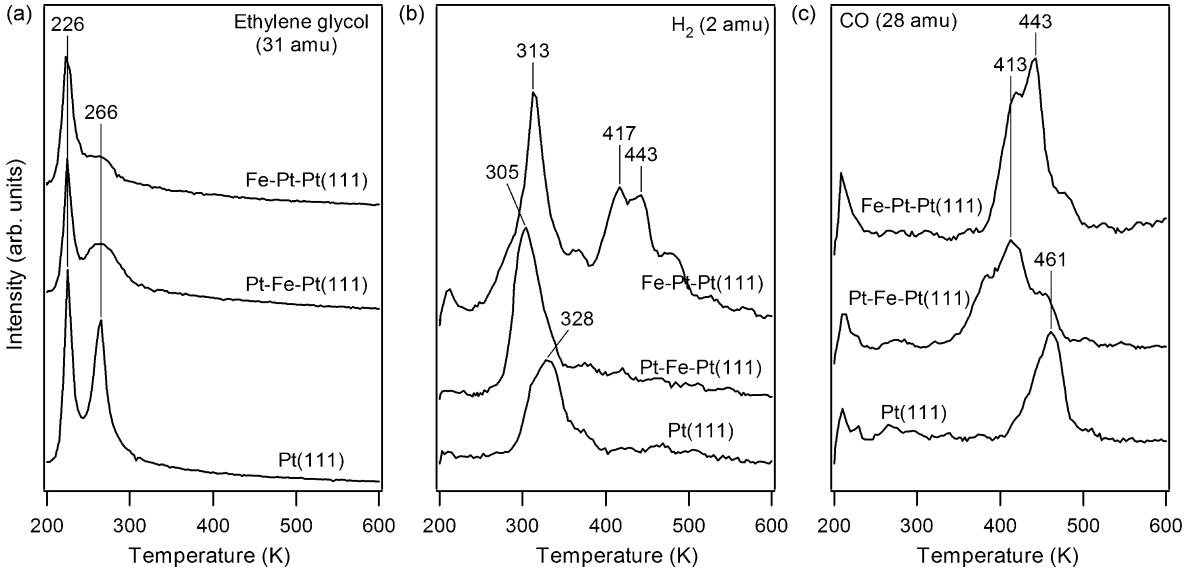

Fig. 2. TPD spectra of (a) ethylene glycol, (b) H_2 and (c) CO following adsorption of 0.2 L ethylene glycol on Fe/Pt(1 1 1) surfaces.

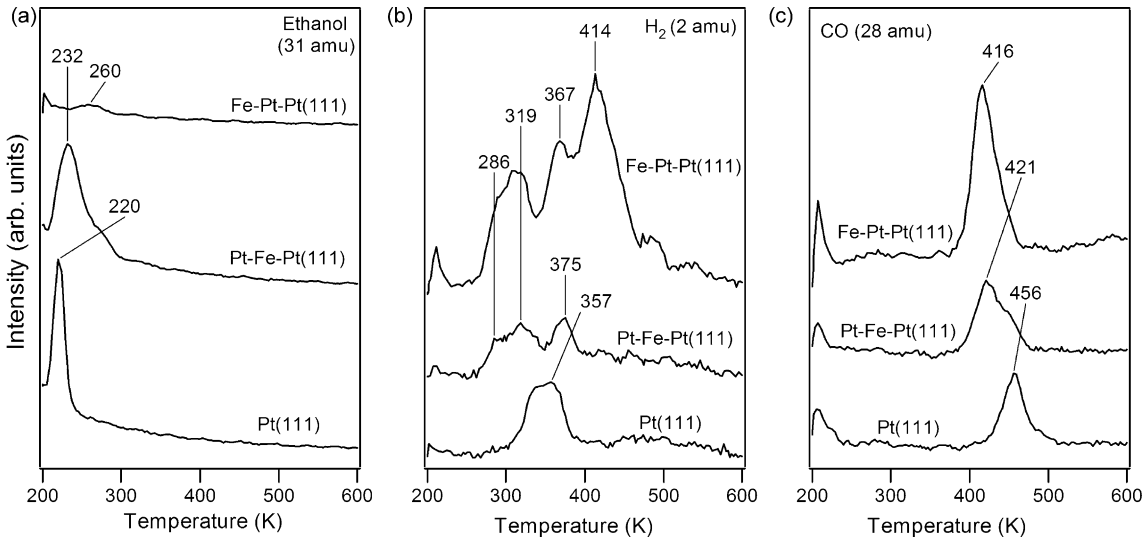

Fig. 3. TPD spectra of (a) ethanol, (b) H_2 and (c) CO following adsorption of 0.3 L ethanol on Fe/Pt(1 1 1) surfaces.

Pt(1 1 1) which occurred at 456 K. Comparing peak areas among the three surfaces, the Fe–Pt–Pt(1 1 1) surface displayed the highest H_2 and CO peak areas, similar to previous results observed on Ni–Pt–Pt(1 1 1) [11]. The Pt–Fe–Pt(1 1 1) surface generated peak areas comparable to Pt(1 1 1).

3.4. Ti/Pt(1 1 1) surface preparation

We have previously studied the preparation and surface characterization of bimetallic surfaces by depositing 3d metals, such as Ni [18,35], Co [34], Fe and Cu [16], on Pt(1 1 1). Similar AES characterization was used in the current study to investigate the deposition of Ti onto Pt(1 1 1) as a function of time, as shown in Fig. 4a. Deposition was carried out at 600 K at 60 s intervals, after which Pt(241 eV) and Ti(421 eV) AES signals were measured. A characteristic break was observed in the Ti(421 eV) AES signal at a deposition time of ~560 s, which was used to mark the formation of a monolayer of Ti on Pt(1 1 1). The corresponding Ti(421 eV)/Pt(241 eV) AES ratio was 2.0.

The stability of Ti on the surface of Pt(1 1 1) was investigated by following the Pt(241 eV) and Ti(421 eV) AES signals as a function of annealing temperature, as shown in Fig. 4b. A monolayer Ti–Pt–Pt(1 1 1) surface was prepared at 300 K, after which the surface was flashed to higher temperatures as indicated and then cooled down for AES measurements. Results showed that the Ti(421 eV) signal remained relatively constant to over 800 K, with a slight decrease over this temperature range, suggesting that Ti remained on or near the surface region and did not diffuse into the subsurface. However, after annealing to temperatures higher than 850 K, the intensity of the Ti(421 eV) feature decreased significantly, suggesting that Ti began to diffuse into the subsurface at these temperatures. At the same time the intensity of the Pt(241 eV) AES signal increased slightly due to decreased screening of Pt atoms by the surface Ti atoms. The results presented here were consistent with previous studies [36] that used He^+ ion scattering spectroscopy (ISS) to probe the topmost layer of Ti films on Pt(1 1 1). Results from that study showed that Ti films were stable on Pt(1 1 1) up to 750–800 K, with Ti atoms starting to diffuse to the subsurface at higher temperatures. The results are also consistent with the literature DFT studies which have shown that the subsurface structure, Pt–Ti–Pt(1 1 1), is preferred in vacuum, while in the presence of O_2 which binds very strongly to Ti, the surface configuration, Ti–Pt–Pt(1 1 1), is favored [37].

Based on these annealing studies, a deposition temperature of 900 K was chosen to prepare the subsurface Pt–Ti–Pt(1 1 1) structure. Preparation of the Ti–Pt–Pt(1 1 1) surface was carried out at 600 K, since at this temperature Ti did not diffuse into the subsurface, but the temperature was high enough to prevent CO adsorption from the background to keep the surface clean during deposition. Compared to previous preparation procedures for Ni/Pt(1 1 1), Co/Pt(1 1 1) and Fe/Pt(1 1 1), the temperature needed to drive Ti atoms into the subsurface was significantly higher. For the other 3d/Pt(1 1 1) bimetallic surfaces, such as Ni, Co, Fe, the subsurface monolayer Pt-3d-Pt(1 1 1) structure could be prepared at 600 K.

3.5. Ethylene glycol TPD on Ti/Pt(1 1 1)

The TPD spectra of (a) ethylene glycol, (b) H_2 and (c) CO following 0.2 L ethylene glycol exposure from Ti/Pt(1 1 1) bimetallic surfaces are compared in Fig. 5. Ethylene glycol desorbed from Ti/Pt(1 1 1) bimetallic surfaces at 263 K, attributed to monolayer desorption, with a lower temperature multilayer peak at 224 K. Ethylene glycol reacted on these surfaces to form H_2 and CO. H_2 desorption occurred from all the surfaces at ~315 K, with a high temperature shoulder at 347 K. The peak temperature was similar to that observed on clean Pt(1 1 1). CO desorbed from 0.5 ML Pt–Ti–Pt(1 1 1) at 434 K, a slightly lower peak temperature compared to clean Pt(1 1 1). From 0.5 ML Ti–Pt–Pt(1 1 1) CO desorption occurred at 389 K and 439 K, both lower than that on Pt(1 1 1). Comparing the different Ti/Pt(1 1 1) bimetallic surfaces, the shift in peak temperature relative to Pt(1 1 1) was not as significant as that on Fe/Pt(1 1 1) and especially Ni/Pt(1 1 1) [11] surfaces. However, consistent with previous results, the surface with Ti atoms on the surface, Ti–Pt–Pt(1 1 1), displayed increased activity compared to the subsurface Ti structure, Pt–Ti–Pt(1 1 1). It is also interesting to note that the differences in activity between surface versus subsurface structures were observed at a coverage of 0.5 ML for Ti, as opposed to previous work which focused on 1 ML coverage of 3d atoms on Pt(1 1 1). Experiments were carried out with both 1 ML (not shown here) and 0.5 ML Ti coverages. The 1 ML Pt–Ti–Pt(1 1 1) and Ti–Pt–Pt(1 1 1) surfaces displayed similar TPD results to each other and to the 0.5 ML Ti–Pt–Pt(1 1 1) structure. This suggests that one cannot drive all the Ti atoms at monolayer coverage to the subsurface with the experimental procedures presented here, and for high coverage some Ti atoms

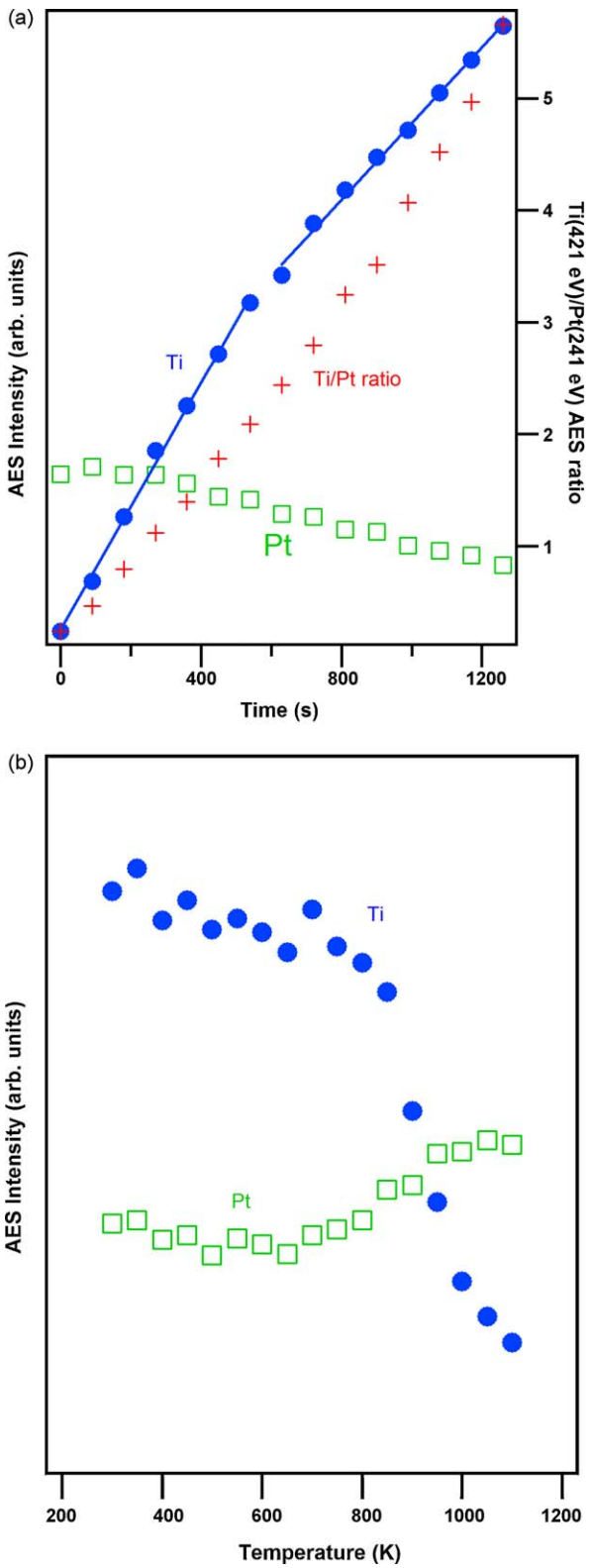

Fig. 4. Intensities of AES Ti(421 eV) and Pt(241 eV) transitions as a function of (a) deposition time and (b) annealing temperature.

remain on the surface, leading to similar activity. On the other hand, on surfaces with a coverage of 0.5 ML, enough Ti atoms diffused into the subsurface to produce a surface with different chemical properties. Another possible explanation for the discrepancy could be inaccuracies in the calibration procedure, in using the break in the AES Ti(421 eV) signal during deposition to mark the formation of a monolayer. Further surface characterization of the Ti/Pt(1 1 1) system is needed to explain some of the differences compared to other 3d/Pt(1 1 1) bimetallic systems.

3.6. Ethanol TPD on Ti/Pt(1 1 1)

The TPD spectra of (a) ethanol, (b) H_2 and (c) CO following 0.3 L ethanol exposure on Ti/Pt(1 1 1) bimetallic surfaces are shown in Fig. 6. Ethanol desorbed from Pt–Ti–Pt(1 1 1) at 223 K, the same peak temperature as from clean Pt(1 1 1). These peaks were attributed to monolayer desorption. On Ti–Pt–Pt(1 1 1), the ethanol peak area was significantly reduced compared to the other surfaces. Ethanol reacted on Ti/Pt(1 1 1) bimetallic surfaces to form H_2 and CO. From Pt–Ti–Pt(1 1 1), H_2 desorbed at 300 K, with a broad second peak at 401 K. From Ti–Pt–Pt(1 1 1), H_2 desorption occurred at 300 K and 435 K. The high temperature peak was reaction-limited on both surfaces. CO desorption occurred at 426 K from both bimetallic surfaces, a slightly lower peak temperature compared to clean Pt(1 1 1). Overall, increased H_2 and CO peak areas were observed on Ti–Pt–Pt(1 1 1) compared to the Pt–Ti–Pt(1 1 1) surface. These results are similar to those for ethylene glycol on Ti/Pt(1 1 1), and to previous results for ethanol on Fe/Pt(1 1 1) and Ni/Pt(1 1 1) [11].

4. Discussion

4.1. TPD quantification of reaction yields

The TPD results have been quantified using a procedure described previously [11]. The saturation coverage of H_2 on Pt(1 1 1) is reported in the literature to be ~0.45 ML (or 0.9 ML $H_{(a)}$) [38] based on D_2 adsorption using nuclear microanalysis. The saturation coverage of CO on Pt(1 1 1) is reported to be 0.68 ML [39]. In the current work, the absolute coverages of H_2 and CO were obtained by comparing their TPD peak areas with those following saturation exposures of H_2 and CO on Pt(1 1 1). Product yields were then calculated from TPD results with appropriate subtraction of the contributions of H_2 and CO accumulated from the UHV background during surface preparation.

Ethylene glycol reacts on 3d/Pt(1 1 1) surfaces by two reactions: (1) reforming and (2) total decomposition.

$$a\mathrm{HOCH_2CH_2OH} \rightarrow 2a\mathrm{CO} + 3a\mathrm{H_2} \quad (1)$$

$$b\mathrm{HOCH_2CH_2OH} \rightarrow 2b\mathrm{C} + 2b\mathrm{O} + 3b\mathrm{H_2} \quad (2)$$

Ethanol reacts on these surfaces by three reactions, (3) reforming, (4) decarbonylation, and (5) total decomposition. The activity for each reaction pathway was determined using the H_2 and CO TPD yields, as described previously for the Ni/Pt(1 1 1) surfaces [11].

$$a\mathrm{CH_3CH_2OH} \rightarrow a\mathrm{CO} + 3a\mathrm{H_2} + a\mathrm{C} \quad (3)$$

$$b\mathrm{CH_3CH_2OH} \rightarrow b\mathrm{CO} + b\mathrm{CH_4} + b\mathrm{H_2} \quad (4)$$

$$c\mathrm{CH_3CH_2OH} \rightarrow 2c\mathrm{C} + c\mathrm{O} + 3c\mathrm{H_2} \quad (5)$$

The reaction yields for ethylene glycol on Fe/Pt(1 1 1) and Ti/Pt(1 1 1) bimetallic surfaces are summarized in Table 1, along with previous results on Ni/Pt(1 1 1) [11]. Comparing the Fe/Pt(1 1 1) surfaces, the Fe–Pt–Pt(1 1 1) surface shows increased reforming yield compared to Pt–Fe–Pt(1 1 1) and clean Pt(1 1 1). The Pt–Fe–Pt(1 1 1) bimetallic surface also displays increased reforming yield compared to clean Pt(1 1 1). This is in contrast to previous results observed on Ni/Pt(1 1 1), where the Pt–Ni–Pt(1 1 1) subsurface configuration was found to be less active than clean Pt(1 1 1). For both Pt–Fe–Pt(1 1 1) and Fe–Pt–Pt(1 1 1) surfaces, the increase in activity does not influence selectivity, as both display relatively

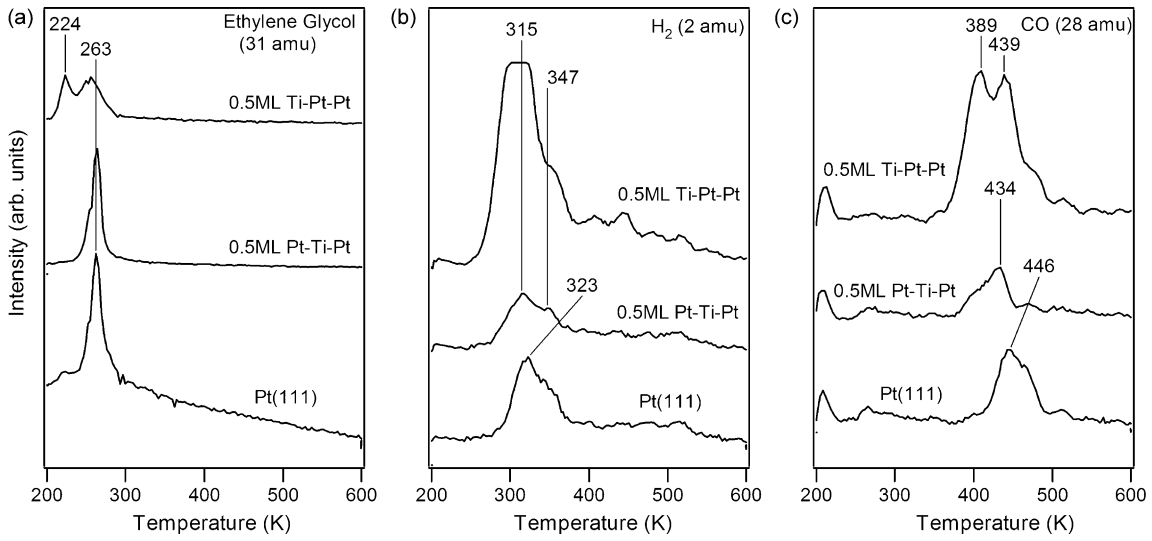

Fig. 5. TPD spectra of (a) ethylene glycol, (b) H_2 and (c) CO following adsorption of 0.2 L ethylene glycol on Ti/Pt(1 1 1) surfaces.

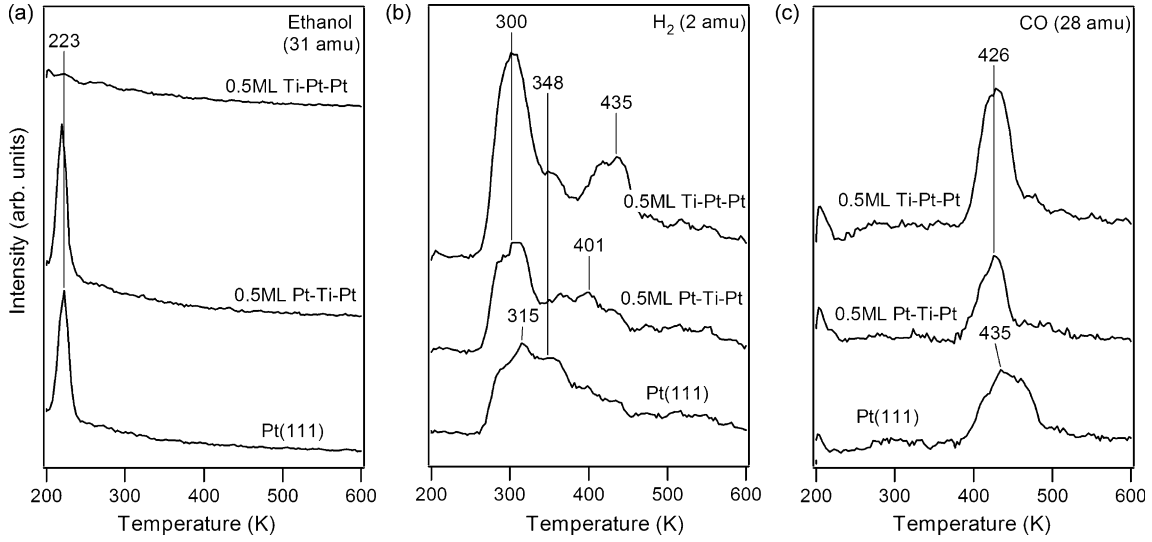

Fig. 6. TPD spectra of (a) ethanol, (b) H_2 and (c) CO following adsorption of 0.3 L ethanol on Ti/Pt(1 1 1) surfaces.

high reforming selectivities comparable to that of clean Pt(1 1 1). Comparing the Ti/Pt(1 1 1) bimetallic surfaces, the surface monolayer Ti–Pt–Pt(1 1 1) displays higher reforming yield compared to Pt–Ti–Pt(1 1 1), while maintaining selectivity similar to Pt(1 1 1). The Pt–Ti–Pt(1 1 1) surface exhibits low reforming selectivity.

The reaction yields for ethanol on Fe/Pt(1 1 1) and Ti/Pt(1 1 1) bimetallic surfaces are summarized in Table 2, along with previous results on Ni/Pt(1 1 1) [11]. The Fe–Pt–Pt(1 1 1) surface displays increased reforming yield as compared to Pt–Fe–Pt(1 1 1) and clean Pt(1 1 1). The Pt–Fe–Pt(1 1 1) reforming yield is higher than that of clean Pt(1 1 1), similar to the trend observed for ethylene glycol. In contrast to ethylene glycol, the increase in the reforming yield for ethanol on Fe–Pt–Pt(1 1 1) is accompanied by a decrease in the reforming selectivity, as the total decomposition reaction becomes more prominent. For the Ti/Pt(1 1 1) bimetallic surfaces, the Ti–Pt–Pt(1 1 1) surface shows increased reforming yield compared to Pt–Ti–Pt(1 1 1) and clean Pt(1 1 1). The reforming activity on Pt–Ti–Pt(1 1 1) is slightly higher than that on Pt(1 1 1). On both Ti–Pt–Pt(1 1 1) and Pt–Ti–Pt(1 1 1), total decomposition has been found to be the major reaction pathway, leading to decreased reforming selectivity. This is attributed to the high affinity of Ti for oxygen that leads to the formation of atomic oxygen on the surface instead of gas-phase CO.

Overall, comparing the trends for Pt-3d bimetallic surfaces the surface monolayer structure, 3d-Pt–Pt(1 1 1), shows increased oxygenate reforming activity compared to the subsurface monolayer structure, Pt-3d-Pt(1 1 1). This trend persists for different

Table 1
Ethylene glycol reaction yields on Fe/Pt(1 1 1) and Ti/Pt(1 1 1) bimetallic surfaces.

Surface	Activity (ML)			Selectivity (%)	
	Reforming	Decomposition	Total	Reforming	Decomposition
Pt(1 1 1)	0.041	0.003	0.043	94	6
Pt–Ni–Pt(1 1 1)[a]	0.025	0	0.025	100	0
Ni–Pt–Pt(1 1 1)[a]	0.144	0.023	0.167	86	14
Thick Ni/Pt(1 1 1)[a]	0.122	0.016	0.138	88	12
Pt–Fe–Pt(1 1 1)	0.080	0	0.080	100	0
Fe–Pt–Pt(1 1 1)	0.107	0.015	0.122	88	12
Pt–Ti–Pt(1 1 1)	0.011	0.018	0.029	38	62
Ti–Pt–Pt(1 1 1)	0.128	0.029	0.157	82	18

[a] Ref. [11].

Table 2
Ethanol reaction yields on Fe/Pt(1 1 1) and Ti/Pt(1 1 1) bimetallic surfaces.

Surface	Activity (ML)				Selectivity (%)		
	Reforming	Decomposition	CH_4	Total	Reforming D	Decomposition	CH_4
Pt(1 1 1)	0.024	0	0.001	0.025	98	0	2
Pt–Ni–Pt(1 1 1)[a]	0.015	0	0	0.015	100	0	0
Ni–Pt–Pt(1 1 1)[a]	0.074	0.003	0.01	0.087	85	3	12
Thick Ni/Pt(1 1 1)[a]	0.07	0	0.001	0.071	98	0	2
Pt–Fe–Pt(1 1 1)	0.044	0	0	0.044	100	0	0
Fe–Pt–Pt(1 1 1)	0.097	0.054	0	0.150	64	36	0
Pt–Ti–Pt(1 1 1)	0.030	0.076	0	0.106	28	72	0
Ti–Pt–Pt(1 1 1)	0.085	0.105	0	0.191	45	55	0

[a] Ref. [11].

metals (Ni, Co, Fe and Ti) and different oxygenates, such as methanol, ethanol, ethylene glycol and glycerol [11,13,14].

4.2. Correlations with d-band center

The reforming yields of ethylene glycol and ethanol on Fe/Pt(1 1 1) and Ti/Pt(1 1 1) bimetallic surfaces are correlated with the calculated d-band centers of these surfaces, as shown in Fig. 7. The surface d-band center was calculated using DFT; the details of the calculations were reported previously [11]. Our previous results on Ni/Pt(1 1 1) bimetallic surfaces are also included for comparison. The surfaces for which the d-band center is located closer to the Fermi level exhibit higher reforming activity. In general, the surface monolayer 3d-Pt–Pt(1 1 1) structure displays increased reforming yield for both ethylene glycol and ethanol compared to the corresponding subsurface monolayer Pt-3d-Pt(1 1 1) configuration. Among the surfaces studied experimentally, the highest reforming yield was observed on Ni–Pt–Pt(1 1 1) for ethylene glycol and on Fe–Pt–Pt(1 1 1) for ethanol. However, several surfaces did not appear to follow the trends. Specifically, Pt–Fe–Pt(1 1 1) and Pt–Ti–Pt(1 1 1) showed higher reforming yields than Pt(1 1 1). Based on the d-band center correlation, either of these two bimetallic surfaces would be expected to be less active than Pt(1 1 1). One possible explanation is that surface segregation of the 3d metal occurred on these surfaces. This could be because diffusion of the more reactive 3d metal to the subsurface was incomplete on the prepared surfaces, or re-segregation to the surface occurred upon adsorption of the reactants. A similar explanation has been offered for the higher than expected activity of Pt–Co–Pt(1 1 1) for reforming of methanol [13].

The reforming selectivity of Fe/Pt(1 1 1) and Ti/Pt(1 1 1) bimetallic surfaces as a function of d-band center is presented in Fig. 8. Previous results on Ni/Pt(1 1 1) [11] surfaces are also included for comparison. Fig. 8 shows that selectivity is fairly high on most of the surfaces for ethylene glycol, with a slight decreasing trend as the d-band center shifts to the Fermi level. On the other hand, the reforming selectivity decreases significantly for ethanol as the d-band center shifts closer to the Fermi level. One possible explanation is that the binding energy of ethanol is too large, leading to total decomposition to produce atomic carbon and oxygen. This is consistent with the Sabatier's principle, which states that a balance in the binding energy of adsorbed species is needed to achieve the desirable reaction products. It is also

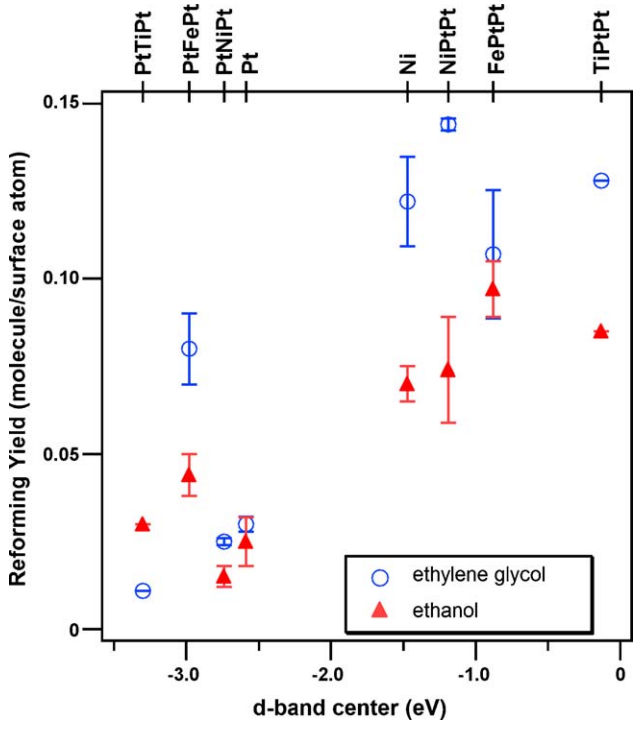

Fig. 7. Ethylene glycol and ethanol reforming yields as a function of d-band center.

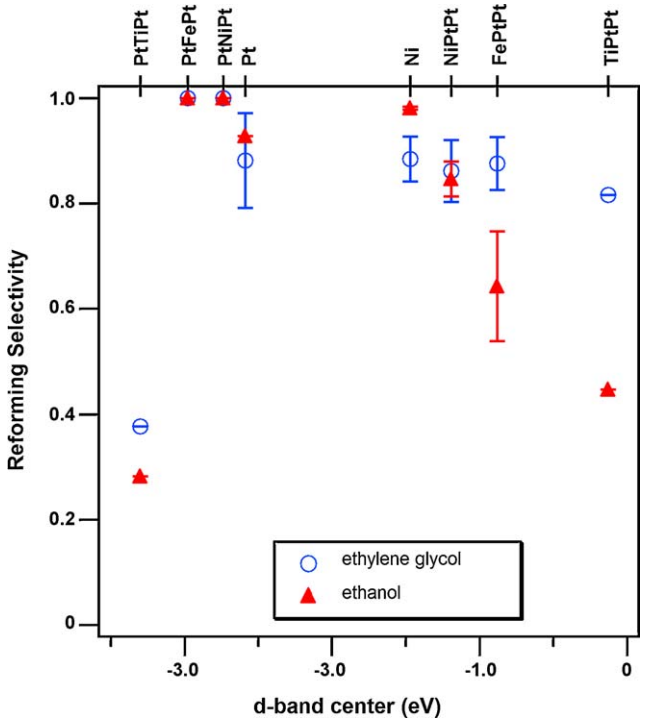

Fig. 8. Ethylene glycol and ethanol reforming selectivities as a function of d-band center.

interesting to note that while ethanol displays decreased reforming selectivity as the surface d-band center moves closer to the Fermi level, the ethylene glycol reforming selectivity remains fairly high. This difference suggests that oxygenates with 1:1 C/O ratios might be more suitable reactants for the production of hydrogen by reforming.

The Pt–Ti–Pt(1 1 1) surface does not follow any of the trends, and displays very low reforming selectivity for both ethylene glycol and ethanol. Further work is needed to understand the properties of this surface, especially surface characterization to confirm that the Ti is driven to the subsurface, forming the ideal Pt–Ti–Pt(1 1 1) surface structure. Overall, the results in Figs. 7 and 8 suggest that 3d-Pt bimetallic surfaces with Ni, Fe as the 3d metal display increased reforming yield compared to Pt(1 1 1) and might be potential catalysts for reforming of oxygenates. However, 3d-Pt surfaces using earlier 3d transition metals such as Ti can lead to decreased selectivity as oxygenates tend to react via total decomposition to produce adsorbed carbon and oxygen on these surfaces.

5. Conclusions

The reactions of ethylene glycol and ethanol have been studied on Fe/Pt(1 1 1) and Ti/Pt(1 1 1) bimetallic surfaces and the following conclusions can be drawn:

(1) The surface monolayer Fe–Pt–Pt(1 1 1) and Ti–Pt–Pt(1 1 1) structures display higher reforming activities for both ethylene glycol and ethanol than the corresponding subsurface monolayer Pt–Fe–Pt(1 1 1) and Pt–Ti–Pt(1 1 1) structures and clean Pt(1 1 1).
(2) The reforming yield displays an increasing trend as the surface d-band center shifts closer to the Fermi level, confirming earlier predictions [11].
(3) The preparation procedure for Pt–Ti–Pt(1 1 1) must be altered from that for the corresponding Pt-3d-Pt(1 1 1) surfaces involving Ni, Co, and Fe, as higher deposition temperatures (900 K compared to 600 K) are required to drive the Ti atoms into the subsurface.
(4) The reforming selectivity of oxygenates, especially ethanol, begins to decrease as the d-band center shifts closer to the Fermi level. This suggests that optimal 3d-Pt catalysts for reforming of oxygenates include Ni, Co, or Fe as the 3d metal, as earlier 3d transition metals can lead to decreased selectivity.
(5) The reactivity trends on Fe/Pt(1 1 1) and Ti/Pt(1 1 1) follow earlier work reported on Ni/Pt(1 1 1) bimetallic surfaces, with 3d-Pt–Pt(1 1 1) surfaces displaying the highest activity. One notable difference between Fe, Ti and Ni-based bimetallic surfaces is the increased activity of Pt–Fe–Pt(1 1 1) and Pt–Ti–Pt(1 1 1) compared to Pt(1 1 1), while the Pt–Ni–Pt(1 1 1) surface is less active than Pt(1 1 1). One possible explanation for the increased activity is the segregation of Fe and Ti atoms from the subsurface region to the surface during reforming reactions.

Acknowledgements

The authors acknowledge financial support from the U.S. Department of Energy, Office of Sciences, Division of Chemical Sciences (Grant FG02-03ER15468).

References

[1] R.R. Davda, J.W. Shabaker, G.W. Huber, R.D. Cortright, J.A. Dumesic, Appl. Catal. B: Environ. 56 (2005) 171–186.
[2] G.W. Huber, S. Iborra, A. Corma, Chem. Rev. 106 (2006) 4044–4098.
[3] S. Wasmus, A. Kuver, J. Electroanal. Chem. 461 (1999) 14–31.
[4] E. Antolini, Mater. Chem. Phys. 78 (2003) 563–573.
[5] H.S. Liu, C.J. Song, L. Zhang, J.J. Zhang, H.J. Wang, D.P. Wilkinson, J. Power Sources 155 (2006) 95–110.
[6] W. Zhou, Z. Zhou, S. Song, W. Li, G. Sun, P. Tsiakaras, Q. Xin, Appl. Catal. B: Environ. 46 (2003) 273–285.
[7] F. Vigier, C. Coutanceau, A. Perrard, E.M. Belgsir, C. Lamy, J. Appl. Electrochem. 34 (2004) 439–446.
[8] J. Mann, N. Yao, A.B. Bocarsly, Langmuir 22 (2006) 10432–10436.
[9] E. Peled, V. Livshits, T. Duvdevani, J. Power Sources 106 (2002) 245–248.
[10] V. Livshits, E. Peled, J. Power Source 161 (2006) 1187–1191.
[11] O. Skoplyak, M.A. Barteau, J.G. Chen, J. Phys. Chem. B 110 (2006) 1686–1694.
[12] O. Skoplyak, M.A. Barteau, J.G. Chen, Surf. Sci. 602 (2008) 3578–3587.
[13] O. Skoplyak, C.A. Menning, M.A. Barteau, J.G. Chen, J. Chem. Phys. 127 (2007) 114707.
[14] O. Skoplyak, M.A. Barteau, J.G. Chen, ChemSusChem 1 (2008) 524–526.
[15] G.W. Huber, J.W. Shabaker, S.T. Evans, J.A. Dumesic, Appl. Catal. B: Environ. 62 (2006) 226–235.
[16] M. Humbert, J.G. Chen, J. Catal. 257 (2008) 297–306.
[17] J.G. Chen, C.A. Menning, M.B. Zellner, Surf. Sci. Rep. 63 (2008) 201–254.
[18] J.R. Kitchen, N.A. Khan, M.A. Barteau, J.G. Chen, B. Yahskinskiy, T.E. Madey, Surf. Sci. 544 (2003) 295–308.
[19] J.R. Kitchin, J.K. Nørskov, M.A. Barteau, J.G. Chen, J. Chem. Phys. 120 (2004) 10240–10246.
[20] J.R. Kitchin, J.K. Nørskov, M.A. Barteau, J.G. Chen, Phys. Rev. Lett. 93 (2004) 156801.
[21] C.A. Menning, H.H. Hwu, J.G. Chen, J. Phys. Chem. B 110 (2006) 15471–15477.
[22] A.M. Goda, M.A. Barteau, J.G. Chen, J. Phys. Chem. B 110 (2006) 11823–11831.
[23] M. Bowker, R.J. Madix, Surf. Sci. 116 (1982) 549–572.
[24] R.J. Madix, T. Yamada, S.W. Johnson, Appl. Surf. Sci. 19 (1984) 43–58.
[25] A.J. Capote, R.J. Madix, J. Am. Chem. Soc. 111 (1989) 3570–3577.
[26] A.J. Capote, R.J. Madix, Surf. Sci. 214 (1989) 276–288.
[27] N.F. Brown, M.A. Barteau, J. Phys. Chem. 98 (1994) 12737–12745.
[28] K.T. Queeney, C.R. Arumainayagam, M.K. Weldon, C.M. Friend, M.Q. Blumberg, J. Am. Chem. Soc. 118 (1996) 3896–3904.
[29] A.F. Lee, D.E. Gawthrope, N.J. Hart, K. Wilson, Surf. Sci. 548 (2004) 200–208.
[30] B.A. Sexton, K.D. Rendulic, A.E. Hughes, Surf. Sci. 121 (1982) 181–198.
[31] K.D. Rendulic, B.A. Sexton, J. Catal. 78 (1982) 126–135.
[32] S.M. Gates, J.N. Russell, J.T. Yates, Surf. Sci. 171 (1986) 111–134.
[33] J. Xu, X. Zhang, R. Zenobi, J. Yoshinobu, Z. Xu, J.T. Yates, Surf. Sci. 256 (1991) 288–300.
[34] N.A. Khan, L.E. Murillo, J.G. Chen, J. Phys. Chem. B 108 (2004) 15748–15754.
[35] B. Frühberger, J. Eng, J.G. Chen, Catal. Lett. 45 (1997) 85–92.
[36] S. Hsieh, D. Beck, T. Matsumoto, B.E. Koel, Thin Solid Films 466 (2004) 123–127.
[37] C.A. Menning, J.G. Chen, J. Chem. Phys. 128 (2008) 164703.
[38] P.R. Norton, J.A. Davies, T.E. Jackman, Surf. Sci. 121 (1982) 103–110.
[39] G. Ertl, M. Neumann, K.M. Streit, Surf. Sci. 64 (1977) 393–410.